94 GHz pulsed coherent radar for high power amplifier evaluation.

Duncan A. Robertson*[1], Robert I. Hunter[1], Thomas F. Gallacher[2]
[1] University of St Andrews, SUPA School of Physics & Astronomy,
St Andrews, Fife KY16 9SS, Scotland
[2] was with Aalto University, School of Electrical Engineering,
Department of Radio Science and Engineering, P.O. Box 13000, FI-00076 AALTO, Finland

ABSTRACT

We present the design and characterization of a 94 GHz pulsed coherent radar to be used for the evaluation and demonstration of novel wideband, high power vacuum tube amplifier technology. The radar is designed to be fully coherent and exploits a low phase noise architecture to maximize Doppler performance. We selected to use horn-fed Fresnel zone plate lens antennas (FZPs) with 4-level phase quantization as a low cost method of realizing large aperture (0.5 m) antennas. The measured performance of these FZPs agrees closely with the design predictions and exceeds that obtainable with a Cassegrain of an equivalent size.

Keywords: Radar, pulsed Doppler, millimeter wave, coherent, high power amplifier, Fresnel zone plate

1. INTRODUCTION

Novel vacuum electronic devices are emerging which will advance the state-of-the art in high power amplification at millimeter wave frequencies. One very promising technology is the gyro-travelling wave amplifier (gyro-TWA) with helically corrugated interaction region (HCIR), currently under development by our collaborators at the University of Strathclyde, Glasgow, Scotland, which offers multi-kilowatt peak power levels over large fractional bandwidths of at least 10%[1,2]. Such amplifiers will open new possibilities for high power, wideband, millimeter wave radars for applications such as remote sensing (e.g. cloud profiling[3]) and space debris monitoring using inverse synthetic aperture radar (ISAR) techniques[4] and in the field of magnetic resonance spectroscopy[5].

We present the design and characterization of a 94 GHz pulsed coherent radar to be used for the evaluation and demonstration of a gyro-TWA wideband, high power amplifier in collaboration with the University of Strathclyde. The radar is designed to be fully coherent and exploits a low phase noise architecture to maximize Doppler performance. The radar has been characterized in low power mode prior to being coupled to the gyro-TWA so that the details of pulse behavior attributable to the high power amplifier can be assessed.

For outdoor demonstrations the radar has been designed with 0.5 m diameter transmit and receive antennas. We selected to use horn-fed Fresnel zone plate lens antennas (FZPs) with 4-level phase quantization as a low cost method of realizing such large aperture antennas. We will show that the measured performance of these low cost FZPs agrees closely with the design predictions and exceeds that obtainable with a Cassegrain of equivalent size.

2. GYRO-TRAVELLING WAVE AMPLIFIER TECHNOLOGY

Many modern high power radars use high power amplifiers rather than oscillators to ensure pulse-to-pulse coherence and be able to exploit advanced coherent pulse processing techniques. At millimeter wavelengths there is lack of amplifier technology delivering kilowatt peak power levels and the most common device is the extended interaction klystron amplifier (EIKA)[6]. These are very mature devices up to ~100 GHz but performance drops off rapidly at higher frequencies and they are typically fairly narrow band devices (~1% bandwidth)[7]. At 94 GHz, an EIKA typically delivers 1 kW peak power over 1 GHz bandwidth, or up to 2 kW peak power narrowband (with an average power of 100 W). In contrast, the gyro-TWA with HCIR is designed to deliver 5 kW peak power over 10 GHz bandwidth at 94 GHz, i.e. a five-fold increase in peak power and a ten-fold increase in bandwidth over that available from an EIKA.

*dar@st-and.ac.uk; phone +44 1334 467307; www.st-and.ac.uk/~mmwave

Radar Sensor Technology XX, edited by Kenneth I. Ranney, Armin Doerry, Proc. of SPIE Vol. 9829
982908 · © 2016 SPIE · CCC code: 0277-786X/16/$18 · doi: 10.1117/12.2223044

Gyro devices are vacuum electronic tubes in which a microwave signal interacts with a gyrating electron beam in a magnetic field using a helically corrugated interaction region to generate or amplify signals at high power levels. They can be configured as oscillators (gyro-backward wave oscillators, gyro-BWOs) or amplifiers (gyro-travelling wave amplifiers, gyro-TWAs). These HCIR-based interaction regions have a unique linear wave dispersion of the microwave signal, which can be readily matched to that of the gyrating electron beam over a very wide frequency range, yielding a very wide bandwidth device. Furthermore, gyro devices offer high efficiencies and very high output powers. Compared to other vacuum tube amplifier technologies (e.g. EIKAs, smooth bore gyro-TWAs, gyro-klystrons), the Strathclyde design offers higher power over wider bandwidth for a lower magnetic field, better scalability to sub-millimeter wave frequencies and reduced mechanical tolerances.

A number of novel gyro devices, operating at the 2nd cyclotron harmonic, have been developed recently at Strathclyde, including a 1 MW X-band gyro-TWA and a gyro-BWO which achieved 10 kW over 91-98 GHz and >4kW from 89-102 GHz[1]. The latter device has now been converted to operate as an amplifier[2] (a gyro-TWA) and it is this device which we aim to demonstrate using our 94 GHz pulsed coherent radar. Fig. 1 shows the 94 GHz gyro-TWA in the lab.

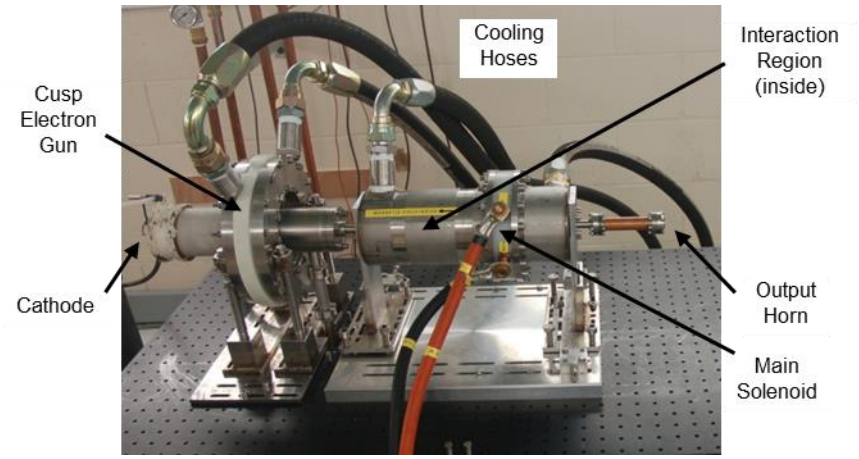

Figure 1: 94 GHz gyro-TWA in lab showing key components. Length ~60 cm.

3. RADAR ARCHITECTURE

To enable testing and demonstration of experimental high power amplifiers, the radar is designed to operate with pulsewidths in the range ~10 ns to ~2 μs, triggered with a variable delay with respect to the amplifier pulsed power trigger. The pulse repetition frequency (PRF) can be varied from ~1 Hz to several kHz, enabling a gradual increase in duty cycle. In practice, the duty cycle will be limited by the gyro-TWA pulsed power supply and cooling requirements.

The overall schematic of the gyro-TWA based pulsed radar experiment is depicted in Fig. 2 (left). The high power amplifier sits in the transmit chain and is driven by a 1.5 W solid-state power amplifier (PA), x6 multiplier and high speed pulse switch. The 15.66 GHz drive signal is provided by the radar circuit which also provides the 94 GHz receive function. For future outdoor experiments, the radar will utilize two 0.5 m diameter Fresnel zone plate (FZP) lens antennas (see Section 5). Fig. 2 (right) shows the radar assembly frame which supports the transmit and receive antennas and the radar circuit. The gyro-TWA, its driver PA, x6 multiplier, pulse switch and pulsed power supply are not shown.

A more detailed block diagram of the radar circuit is given in Fig. 3. The radar uses a heterodyne architecture with an IF at 2.4 GHz. Both transmit and receive local oscillator signals are generated via x6 frequency multipliers. Two modes of operation are indicated: firstly the high power mode when using the gyro-TWA as described above, and secondly a low power mode for characterization prior to high power testing which uses a different low power x6 transmit multiplier. A 15.26 GHz stable local oscillator (STALO) provides the direct input to the receive x6 multiplier. The transmit drive signal is generated by upconverting 400 MHz onto the STALO and is fed as a CW 15.66 GHz signal to the high speed pulse switch in the transmit chain. Demodulation of the 2.4 GHz IF is done with an I-Q mixer driven by a 2.4 GHz phase locked cavity resonator oscillator (PLCRO). The 400 MHz signal is derived from the PLCRO using frequency dividers. Both the STALO and PLCRO are phase locked to a master 10 MHz reference oscillator. Pulses are monitored at 15 GHz with a coaxial tunnel diode and at 94 GHz prior to high power amplification with a waveguide Schottky detector.

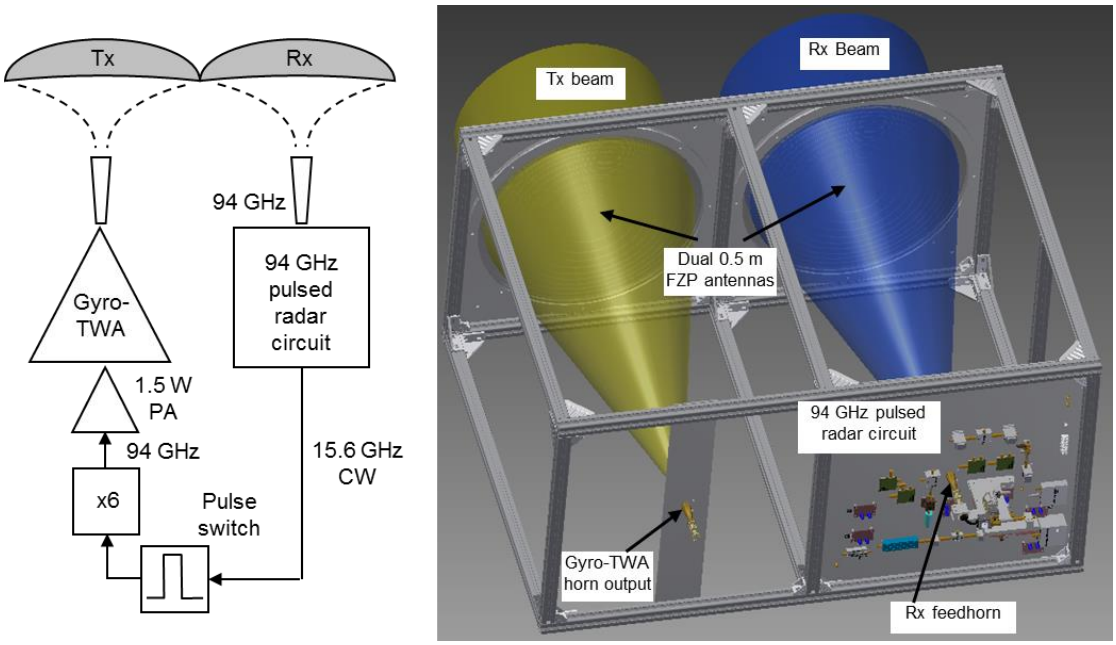

Figure 2: Overall schematic diagram of 94 GHz pulsed radar experiment using gyro-TWA (left), and CAD model showing twin 0.5 m FZP antennas and pulsed radar circuit mounted on frame (right) – N.B. gyro-TWA, driver PA, x6 multiplier and pulse switch not shown.

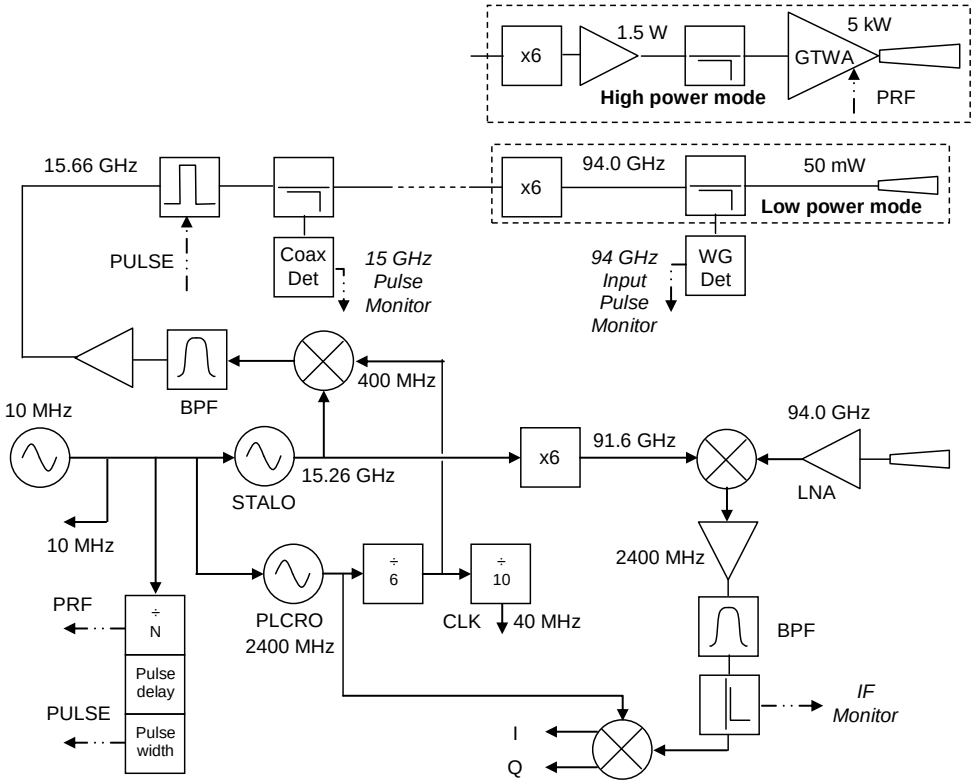

Figure 3: Block diagram of 94 GHz pulsed coherent radar indicating low power mode for testing and high power mode when using the gyro-TWA.

In addition to the RF circuit topology described above, for fully coherent operation the PRF and signal sampling clock must also be coherently related to the carrier phase. The PRF signal is thus derived from the 10 MHz reference by integer division in a programmable microcontroller circuit which provides the settable PRF values. Data acquisition can either be done using a sampling card clocked at 40 MHz derived by division of the 400 MHz signal, or from the 10 MHz reference directly. For testing, a digital oscilloscope can be used which is referenced to the 10 MHz oscillator.

Signals are coupled to free-space using corrugated feedhorns. The receiver and low power transmit chain both use 20 dBi corruagted horns with a sine-squared-parallel internal profile[8]. In high power mode, the gyro-TWA uses an integral feedhorn behind the output vacuum window. As the gyro-TWA output is circularly polarized, the receive chain includes a waveguide polarizer prior to the LNA.

4. PULSED RADAR CHARACTERIZATION

The radar has been characterized in low power mode prior to testing with the high power amplifier. Hence the relative effect of introducing the high power amplifier into the system can be determined and the details of pulse behavior specifically attributable to the high power amplifier can be assessed.

The noise figure of the receiver was measured using the Y-factor method with absorbing loads at 290 and 77 K, the latter cooled with liquid nitrogen. The measured noise figure was determined to be 5.0 dB which is close to that specified for the 26 dB gain low noise amplifier (LNA) of 4.5 dB and accounting for the slight loss of the feedhorn and waveguide polarizer (estimated to be <0.5 dB). With the gains and losses of all the components in the receive chain characterized it was also possible to confirm that the noise power spectral density at different points in the system (e.g. the 2.4 GHz IF monitor or the I-Q outputs) is consistent with the noise figure, accounting for the signal architecture.

The transfer characteristics of the LNA, 94 GHz mixer, IF amplifier and I-Q mixer were characterized to confirm their gains/losses and identify the points at which they exhibit gain compression. This information led to the optimization of the total amount of IF gain depending on the overall magnitude of signals being received. For the maximum sensitivity when observing small signals, a high IF gain permits measurements down to the receiver front end noise floor but the receiver compresses in the IF amplifier. For maximum signal handling when receiving large signals, the IF gain must be lowered such that compression is set by the front end LNA. With 17 dB IF gain, the compression points of the four key components listed above are approximately coincident so this represents the minimum IF gain for optimum receiver performance. Baseband amplification of the I-Q signals has not been implemented thus far but will be required to optimize the measurement dynamic range when using the data acquisition card.

The phase noise of the radar has not been measured directly but is expected to be dominated by the phase noise of the 15.26 GHz STALO which is a phase locked dielectric resonator oscillator (PLDRO), locked to the 10 MHz ovenized crystal oscillator. The STALO has a phase noise performance of -90, -112, -118, -119 & -139 dBc/Hz at offsets of 100, 1k, 10k, 100k & 1M Hz respectively.

The pulse fidelity of the radar was characterized by injecting the attenuated transmit signal directly into the receive LNA via a waveguide rotary vane attenuator. The following results were obtained with a 94 GHz signal level into the LNA of -30 dBm. The received pulse spectrum was observed at the 2.4 GHz IF monitor point on a spectrum analyzer and is shown in Fig. 4 for a pulsewidth of 200 ns and a PRF of ~4 kHz. The spectrum is very clean and symmetric and exhibits the classic sinc response of a pulsed waveform with a mainlobe width of 10 MHz and subsequent lobes of 5 MHz width, as expected for a 200 ns pulsewidth, and first sidelobes at -13 dBc.

The pulse characteristics were assessed in the time domain using a 600 MHz bandwidth 4-channel digital oscilloscope which measured the 15 and 94 GHz detector outputs and the I-Q outputs. An example plot of the pulse shapes is shown in Fig. 5 for a pulse width of 200 ns. It is clear that the pulse fidelity of the radar is excellent with the two monitor pulses showing very fast rise and fall times of order ~1 ns thanks to the use of the high speed switch at 15 GHz and the pulse sharpening threshold effect of the transmit x6 multiplier. The pulse tops are very flat suggesting negligible power variation during a pulse. The I-Q outputs are also very clean, again showing good flatness across the pulse. A minor amount of ringing lasting <10 ns is evident on the rising and falling edges of the I-Q outputs. The pulse shapes are completely steady with time and the I-Q balance is also very stable, only showing any drift if the radar or transmit multiplier is still warming up.

Finally, the phase response of the radar was verified by adding a waveguide rotary phase shifter to the LNA input and observing the I-Q outputs with 100% persistence on the oscilloscope as the phase shifter was varied through one cycle of

phase at 94 GHz. This is shown in Fig. 5 (right) and confirms the pulse shape and flatness is maintained as the phase balance cycles between I and Q outputs.

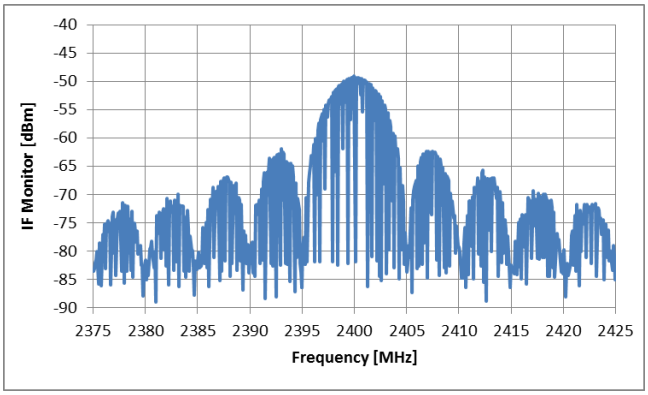

Figure 4. Pulse spectrum measured at IF monitor point for a directly injected, attenuated 94 GHz transmit signal. The pulsewidth was 200 ns and the PRF was ~4 kHz.

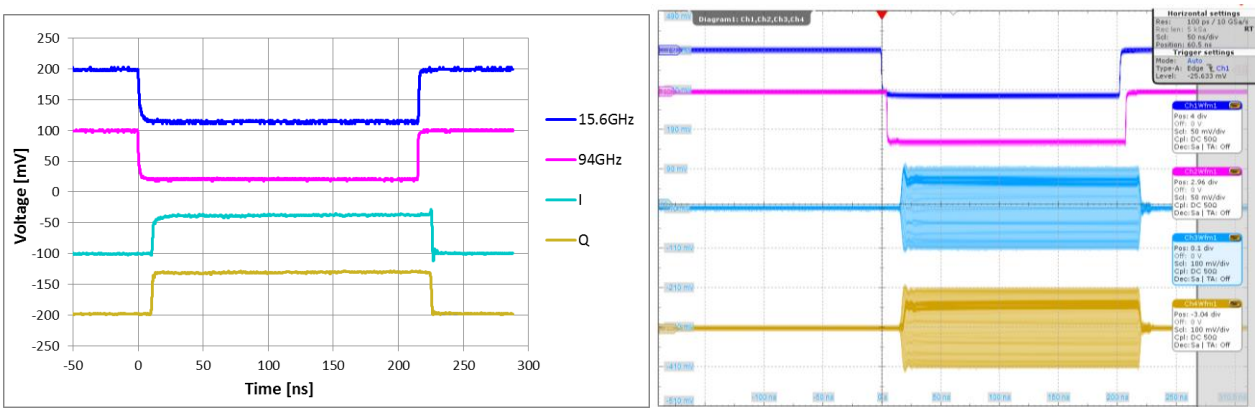

Figure 5. Time domain pulse shapes for a 200 ns pulse measured at the 15 and 94 GHz detectors and I-Q outputs (left). The effect of varying the phase of the received signal over a whole cycle is observed in the I-Q outputs (right).

5. FRESNEL ZONE PLATE ANTENNAS

For future outdoor demonstrations of the high power radar we aim to demonstrate it in a cloud profiling experiment. Ground-based cloud profiling radars typically use twin zenith pointing antennas of high gain / narrow beamwidth; at 94 GHz these would likely be 0.5 to 1.0 m in diameter. The most common type of high gain antenna at 94 GHz is the Cassegrain but these are very expensive in such large diameters and often have fairly modest sidelobe performance of only -18 to -20 dB. However, they do have the advantage of having a short focal distance, or F-number, for their diameter. In our case we did not have a particular space constraint so to realize a low-cost 0.5 m antenna we selected to design a Fresnel zone plate (FZP) lens antenna, fed by a corrugated feedhorn. This also has the advantage of having better sidelobe performance than a similar sized Cassegrain.

The FZP is a classic diffractive optical element which approximates the phase transformation behavior of a lens using discretized phase steps rather than a continuous profile to match the phase curve of the impinging wave[9]. This can be achieved with two approaches: one utilizing alternate transmitting and blocking zones (known as the Soret zone plate) and the other utilizing a stepped dielectric material with alternating zones or varying thickness yielding a relative phase difference (known as the Wood zone plate). We selected the phase reversing Wood zone plate (WZP) design and utilized a 4-level phase-step, or “quarter-wave”, design for higher antenna efficiency. In practice, this structure is achieved by machining stepped concentric grooves in one side of a disc of suitable dielectric material.

There exists no closed form solution for the optimization of quarter-wave grooved WZPs so we performed a physical optics design using the Fresnel-Kirchhoff diffraction integral which accounts for the multi-level phase quantization and base thickness effects[10]. The illuminating feed was a 20 dBi corrugated feedhorn with a sine-squared-parallel profile whose phase center is at the horn aperture[8]. The choice of dielectric material for the WZP was dictated by ease of machining and the availability in sheets of specific thicknesses identified as being optimal for maximizing gain. Polycarbonate was selected as the preferred material given its low cost, availability in large diameters and ease of manufacturing. Whilst polycarbonate is intrinsically lossier than common lens materials such as HDPE or Rexolite, the realized loss is very low due to the small thickness of the zone plate. Table 1 shows the design parameters for the WZPs.

Table 1. Design parameters for the Wood zone plate antennas.

Parameter	**Value**	**Units**
Aperture diameter	500	mm
Permittivity	2.76 + 0.019j	
F-number	1.76	
Input focal length	879	mm
Feed beamwaist	4.02	mm
Edge taper	-11	dB
Overall thickness	8	mm
Groove depths	0, 1.21, 2.42, 3.63	mm
Base thickness	4.37	mm

The far-field patterns of the WZP were measured on an outdoor test range with a remote transmitter positioned just beyond the far-field distance at a range of 160 m. The WZP with feed assembly and heterodyne receiver were mounted on a computer-controlled turntable. Received signals were measured with a spectrum analyzer and collected as a function of azimuth angle. The measured patterns are shown in Fig. 6 along with the simulated design predictions obtained using the modelling approach mentioned above.

The measured E- and H-plane far-field patterns agree extremely well with theory out to the third sidelobes below -35 dB. Further off-axis, the general trend agrees well with predictions but there are some discrepancies from theory believed to be due to machining tolerances on the groove dimensions. The mainlobe is very symmetrical with measured 3 dB beamwidths of 0.43° in both E- and H-planes and a peak sidelobe level of -25 dB. The measured gain is close to the predicted value of 52 dBi within experimental error (with a simulated aperture efficiency of 79%). When used in the radar, these antennas will yield a two-way beamwidth of 0.30° and sidelobe level of -50 dB.

These results demonstrate that millimeter wave large aperture Fresnel zone plate antennas can offer higher performance than Cassegrains of a similar size, for a fraction of the cost, albeit occupying a greater volume. Note that shorter F-number and hence more compact WZP designs are feasible but we made the decision to base our design on the availability of an existing feedhorn. In addition, compared to a conventional curved-surface lens, the WZP is much lighter and simpler to machine.

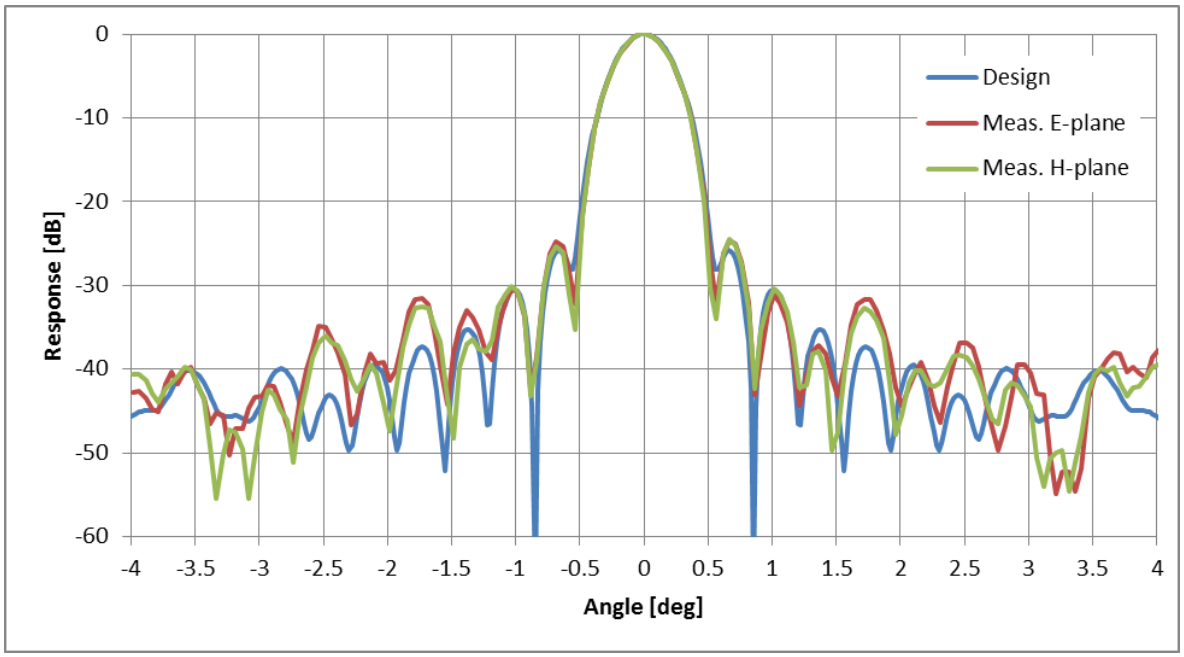

Figure 6. Measured E- and H-plane far field patterns for 0.5 m diameter FZP at 94 GHz versus design.

6. DISCUSSION & CONCLUSIONS

We have presented the design and characterization of a 94 GHz pulsed coherent radar to be used for the evaluation and demonstration of novel wideband, high power vacuum tube amplifier technology, specifically the gyro-travelling wave amplifier with helically corrugated interaction region being developed by our partners at the University of Strathclyde. The gyro-TWA offers to deliver 5 kW peak power over 10 GHz bandwidth at 94 GHz, a factor of 50x more power:bandwidth product than that available from an EIKA.

The radar is fully coherent and aims to maximize Doppler performance being based around a low phase noise 15 GHz STALO which is phase locked to a 10 MHz reference. The radar uses a heterodyne architecture with an IF at 2.4 GHz. Both transmit and receive local oscillator signals are generated via x6 frequency multipliers. Demodulation of the IF is done with an I-Q mixer driven by a 2.4 GHz oscillator which is also phase locked to the 10 MHz reference. Pulse width, pulse trigger delay and PRF are all adjustable. Low power testing is achieved using a low power transmit multiplier. High power testing of the gyro-TWA will be achieved using a 1.5 W solid state 94 GHz driver amplifier.

In low power mode, the radar exhibits excellent performance with a 5 dB noise figure, IF gain which can be optimized for either large signal capability or maximum sensitivity, very good pulse fidelity (~1 ns rise/fall times and flat pulse amplitude), and excellent I-Q phase stability. When the gyro-TWA is incorporated the radar will be used to evaluate the detailed pulse behavior attributable to the high power amplifier.

For future outdoor testing we have designed, manufactured and characterized a pair of 0.5 m Fresnel zone plate lens antennas which achieve 3 dB beamwidths of 0.43° in both E- and H-planes and a peak sidelobe level of -25 dB. The measured gain is close to the predicted value of 52 dBi. The horn-fed FZP, whilst bulkier than a Cassegrain, offers easier manufacture, lower sidelobe level and comparable efficiency, but at a fraction of the cost.

7. ACKNOWLEDGEMENTS

The authors thank our collaborators at the University of Strathclyde and Alistair Moore for building power supply electronics. We acknowledge the funding received from the Science and Technology Facilities Council which has supported this work under grants ST/K006703/1 and ST/N002318/1.

REFERENCES

[1] W. He, C.R. Donaldson, L. Zhang, K. Ronald, P. McElhinney and A.W. Cross, "High power wide-band gyro-BWO operating towards the terahertz region", Phys. Rev. Lett., 110, 165101, 2013.

[2] W He, C.R Donaldson, L. Zhang, P. McElhinney, K. Ronald and A.W. Cross, "W-band Gyro-TWA using a Cusp Electron Gun and a Helically Corrugated Interaction Region", 2013 IEEE 14th International Vacuum Electronics Conference, IVEC 2013, Paris, France, 21st to 23rd May, 2013.

[3] Kollias, P., E.E. Clothiaux, M.A. Miller, B.A. Albrecht, G.L. Stephens, and T.P. Ackerman, "Millimeter-Wavelength Radars: New Frontier in Atmospheric Cloud and Precipitation Research". Bull. Amer. Meteor. Soc., 88, pp. 1608–1624, 2007.

[4] M.G. Czerwinski & J.M. Usoff, "Development of the Haystack Ultrawideband Satellite Imaging Radar", Lincoln Lab Journal, Vol. 21, No. 1, pp. 28 - 44, 2014

[5] P.A.S. Cruickshank, D.R. Bolton, D.A. Robertson, R.I. Hunter, R.J. Wylde & G.M. Smith, "A kilowatt pulsed 94 GHz electron paramagnetic resonance spectrometer with high concentration sensitivity, high instantaneous bandwidth, and low dead time", Rev. Sci. Instrum. 80, 103102, 2009.

[6] Communications & Power Industries: http://www.cpii.com/product.cfm/7/40

[7] D. Berry, H. Deng, R. Dobbs, P. Horoyski, M. Hyttinen, A. Kingsmill, R. MacHattie, A. Roitman, E. Sokol & B. Steer, "Practical Aspects of EIK Technology", IEEE Trans. Electron Devices , Vol. 61, No. 6, pp. 1830 - 1835, 2014.

[8] J. McKay, D.A. Robertson, P.A.S. Cruickshank, R.I. Hunter, D.R. Bolton, R.J. Wylde, & G.M. Smith, "Compact Wideband Corrugated Feedhorns With Ultra-Low Sidelobes for Very High Performance Antennas and Quasi-Optical Systems", IEEE Trans. Antennas and Propagation, Vol. 61, No. 4, pp. 1714 – 1721, 2013.

[9] H. Hristov, Fresnel zones in wireless links, zone plate lenses and antennas, Artech House, 2000.

[10] T.F. Gallacher, "Optoelectronic modulation of mm-wave beams using a photo-injected semiconductor substrate", PhD thesis, University of St Andrews, 2012.